

Deuteron and proton magnetic resonance in *a*-Si:(D,H)

D. J. Leopold

Department of Physics, Washington University, St. Louis, Missouri 63130

J. B. Boyce

Xerox Palo Alto Research Center, Palo Alto, California 94304

Peter A. Fedders and R. E. Norberg

Department of Physics, Washington University, St. Louis, Missouri 63130

(Received 19 July 1982)

Deuteron and proton NMR measurements have been made on a plasma-deposited *a*-Si:(D,H) sample. The spin-lattice relaxations include resolvable contributions arising from relaxations which proceed via molecular orthohydrogen and paradeuterium impurities. Several alternate relaxation mechanisms are considered. The deuteron resonance shows two distinct components, one of which exhibits a long spin-lattice relaxation time T_1 and a 66-kHz quadrupole-split resonance doublet line shape, which is shown to be characteristic of D bonded to Si.

I. INTRODUCTION

Deuteron magnetic resonance (DMR) provides a particularly useful method for the study of condensed matter because DMR often permits identification of resolvable contributions from the single-spin quadrupole interactions of spins in different environments. Comparisons of both DMR and proton NMR results in the same sample offer an additional opportunity for understanding the details of spin-lattice relaxation and resonance line shapes in terms of the internal structure and dynamics of the sample material.

In this paper we report pulsed DMR in plasma-deposited *a*-Si:(D,H) and compare the results with our own and other proton NMR studies in an effort to understand the structural role of hydrogen in amorphous silicon. Deuteron T_1 (spin-lattice) and T_2 (transverse) relaxation times were measured as functions of temperature at several Larmor frequencies. There is a DMR T_1 minimum for a narrow-line 3-at. % D component of a two-phase resonance line shape. This narrow signal arises from the weakly bound deuterium (WBD) fraction. Protons also show a T_1 minimum for both broad and narrow components in this sample and in others. These T_1 minima are shown to reflect D and H spin diffusion to a dilute array of trapped fast-relaxing molecular *p*-D₂ and *o*-H₂ impurities.¹⁻³ Ortho-to-para conversion experiments reported⁴ on *a*-Si:H

have shown such T_1 minima to increase upon holding the sample at liquid-helium temperatures for several weeks.

Fourier-transform line shapes were obtained from deuteron free-induction decays and quadrupole echoes. The transforms show a sharply resolved 21-at. % D temperature-independent quadrupole-split resonance doublet with 66-kHz splitting. This component is interpreted to be a tightly bound deuterium (TBD) species and shows a T_1 of the order of minutes rather than the seconds characteristic of the narrow DMR component. The quadrupole splitting may reduce the spin-diffusion rate and render the molecular *p*-D₂ T_1 pathway ineffective for the TBD component. The well-defined quadrupole splitting indicates rather homogeneous configurations for TBD in amorphous silicon and is in agreement with reported⁵ infrared observations of stretching mode vibrations in *a*-Si:(D,H). DMR provides a sensitive structural probe of hydrogenated amorphous silicon and gives rise to a clear distinction between the two separated phases often deduced^{6,7} from proton NMR.

II. EXPERIMENTAL PROCEDURE

Two-pulsed NMR spectrometers were employed in studying the temperature dependence of T_1 and T_2 relaxation times for deuterons and protons in *a*-

Si:(D,H). Low-field measurements were made in a 23-kG Varian electromagnet with a helium-gas-flow cryoprobe used for temperature variation. Also a 46-kG superconducting solenoid was used for high-field measurements with a vacuum-insulated sample probe immersed in a liquid-helium bath providing low-temperature capabilities. Temperature regulation was accomplished in each case with a commercial unit using a current-controlled resistance wirewound heater with temperature feedback from a carbon glass sensor and thermocouple. Temperature control could be maintained with either system to within ± 0.1 K for several hours.

A frequency synthesizer was used to generate the rf, which was gated and amplified to achieve the short pulse widths needed for broad-line studies in solids. Typical pulse widths for these experiments were a few microseconds. A phase-sensitive receiver was used to detect the free-induction decay or echo following the pulses. Signal-to-noise ratios were improved by digitally averaging many sweeps with the use of a Biomation transient recorder and computer or Nicolet signal averager. 1024-point Fourier transforms of the transients were performed by computer to study line shapes as a function of temperature. Quadrupole echoes were obtained with the use of a $90^\circ\text{-}\tau\text{-}90^\circ$ pulse sequence with the second pulse phase shifted by 90° . T_1 measurements were done using both an inversion-recovery two-pulse sequence and a repetition-rate method. Deuteron NMR measurements were obtained at the Larmor frequencies 14.4 and 30.0 MHz and compared with proton measurements at 14.4 and 91.8 MHz.

The α -Si:(D,H) sample studied was prepared⁸ by 18-W rf plasma deposition from a 5% silane and 95% molecular deuterium gas mixture onto the cathode room-temperature substrate. The details of sample preparation are reported elsewhere.⁸ In fact, the sample was one of those used previously by Reimer, Vaughan, and Knights⁹ to study deuterium dilution effects on the proton resonance.

From our H_2O and D_2O spin-count comparisons we found a total of 7-at. % hydrogen and 24-at. % deuterium in the α -Si:(D,H) sample. These spin-count measurements were found to be constant from liquid-helium temperatures up to room temperature.

III. OUTLINE OF RESULTS FOR DEUTERON RELAXATION

Some of our deuteron NMR (DMR) results in the α -Si:(D,H) sample are summarized in Fig. 1. For

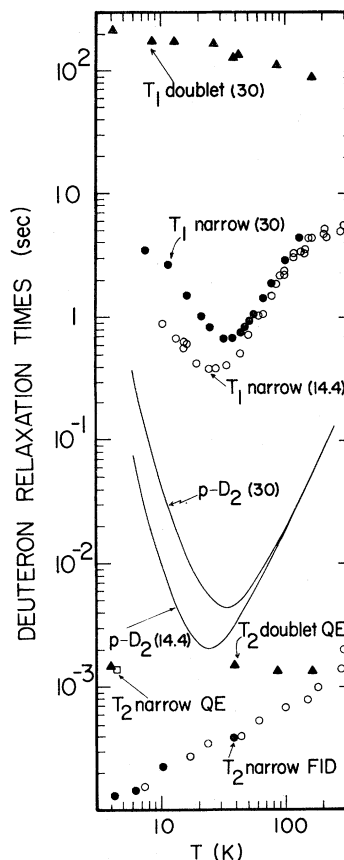


FIG. 1. Deuteron relaxation times in α -Si:(D,H). In the upper half of the figure are spin-lattice relaxation times T_1 for the doublet component (triangles) and the narrow component (dots for 30.0 MHz and circles for 14.4 MHz). Below are relaxation times T_2 from doublet quadrupole echo envelopes (triangles) and from narrow-component measurements including 14.4-MHz free-induction decays (circles), 30.0-MHz free-induction-decay Fourier transforms (dots), and a single 30.0-MHz quadrupole echo envelope (square). The curved lines indicate $T_1(\text{D}_2)$ calculated for deuterons in isolated $p\text{-D}_2$ molecules in a solid nonmagnetic host at 14.4 and 30.0 MHz.

purposes of clarity in the figure, some neighboring data points have been averaged. An NMR spin-count calibration comparison with D_2O shows that there is a 3-at. % D narrow-line component with a T_2 ranging from 2 msec at 300 K down to 130 μsec at 4.2 K. This narrow-line component, which we associate with the WBD regions of the sample, has a spin-lattice relaxation that shows clear T_1 minima at 25 and 34 K (for 14.4 and 30.0 MHz, respectively). The spin-lattice relaxation of this component is dominated by spin diffusion to molecular $p\text{-D}_2$ relaxation centers richly distributed (shown later to be

~ 700 ppm) throughout the sample. The lines drawn in Fig. 1 show the T_1 for deuterons in dilute molecular p -D₂ calculated¹⁰ for 14.4 and 30.0 MHz with local electric field gradients assumed to have no symmetry and the parameter $r=0$. The characteristic temperature has been taken to be $\Theta_c=40$ K. These were the parameters found to fit the relaxation of dilute o -H₂ in rare-gas solids¹¹ and also used earlier¹ in α -Si:H. The temperature of the 14.4-MHz T_1 minimum has been taken to be 25 K. The calculated minimum T_1 value depends only on the Larmor frequency and on the assumed symmetry.

There also is a larger fraction 21-at. % D component with long T_1 and a quadrupolar 66-kHz Pake doublet observed on both free-induction decays and quadrupole echoes. We associate this signal with the TBD fraction of the sample. Its very distinctive long T_1 (90–220 sec) may arise from the effective elimination of p -D₂ molecules as relaxation centers since the quadrupolar doublet splitting greatly reduces the deuteron spin-diffusion rate. The product M_0T was found to be independent of temperature over the range of the measurements for both the narrow-line and the doublet DMR components.

Figure 2 shows an example of the large difference between the T_1 components at 26 K. The sample is investigated via free-induction decays following 90° pulses applied at various repetition rates. Each trace shown is the digital average of eight free-induction decays. The full sweep length displayed is 1 msec. At a pulse repetition interval of 30 sec the doublet component is greatly reduced from that for a 10-min interval. The decay of the narrow unsplit line remains virtually unchanged until repetition intervals shorter than 1 sec.

Thus, deuteron NMR yields a much greater distinction between the hydrogen configurations in α -Si than has been obtained from proton NMR. The principal goal of the present paper is to understand the relaxation data of Fig. 1 and their implications for the structure and dynamics of deuterium in amorphous silicon.

IV. SPIN-RELAXATION PROCESSES

We have investigated three distinct mechanisms for the T_1 relaxation of H and D nuclear spins in α -Si:(D,H). In all of these mechanisms the nuclear magnetization diffuses to dilute H₂ or D₂ molecules and ultimately relaxes via the electronic shell of the molecule. The electric quadrupole-quadrupole

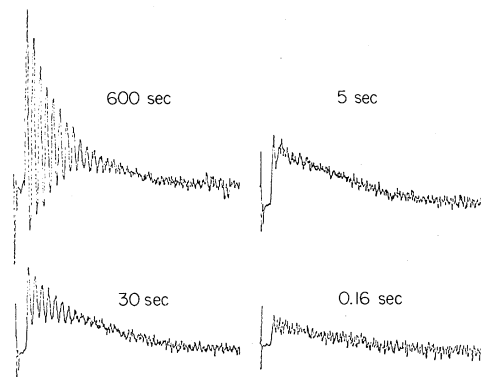


FIG. 2. 30.0-MHz DMR free-induction decays for several repetition intervals at 26 K. The sweep length is 1 msec. As the pulse repetition interval is decreased, the doublet component saturates out well before the narrow component changes significantly.

(EQQ) coupling among the o -H₂ and p -D₂ molecules probably can be neglected¹¹ since the molecular hydrogen concentration will be found to be less than 700 ppm, and also since the static field gradients at molecular hydrogen sites in α -Si may give rise to crystal-field splittings much larger than EQQ. These mechanisms are as follows.

(i) In the first relaxation mechanism the H (D) nuclear magnetization diffuses to the nuclear spins of H₂ (D₂) molecules. The magnetization of the H₂ (D₂) nuclei then relaxes¹⁰ to the electronic part of the molecule and ultimately to the lattice. The second step corresponds to the relaxation of nuclear magnetization for dilute molecular o -H₂, which has been examined¹¹ for dilute hydrogen in rare-gas solids. The two-step process has been discussed in the literature previously¹ with respect to H₂ in α -Si:H and will be used extensively in Sec. V of the present paper to describe the observed relaxation of both H and D with T_1 minima between 0.4 and 2 sec. In their ground states both o -H₂ and p -D₂ have $J=1$, the same electron distributions, and thus the same coupling to the lattice. Since the molecules both have $I=1$ the difference between their nuclear relaxation rates at the same Larmor frequency arises from their different masses and intramolecular coupling coefficients. Molecular HD and the $I=2, J=0$ fraction of o -D₂ can be neglected as relaxation centers since their intrinsic nuclear relaxation times are long.

(ii) In the second relaxation mechanism the H (D) nuclear magnetization diffuses to some H (D) atoms that are near to H₂ (D₂) molecules. Then, those H (D) nuclear spins relax directly to the H₂ (D₂) elec-

tronic shell via the dipolar interaction without going through the intermediary of the H_2 (D_2) nucleus. The calculation for the relaxation rate associated with the last step of this process is very similar to the standard calculation¹² for spin relaxation via paramagnetic impurities. After averaging over angles, one obtains the rate

$$R = \frac{1}{\hbar^2} (\gamma_n \gamma_m \hbar^2 / r^3)^2 [2I(I+1)/5] \times [F(\omega_0) + 8F(\omega_0 + \omega_m) + \frac{1}{3}F(\omega_0 - \omega_m)], \quad (1)$$

where I is the spin of the H (D) nuclear spin, γ_n and γ_m are the gyromagnetic ratios of the H (D) nuclear spin and the H_2 (D_2) molecular spin, respectively, ω_0 and ω_m are Larmor frequencies of the nuclear and molecular spins, respectively, and r is the distance between the H (D) and the H_2 (D_2) molecule. The quantity $F(\omega)$ is the spectral function for the molecular spin

$$F(\omega) = \Gamma_p / (\omega^2 + \Gamma_p^2), \quad (2)$$

where Γ_p is the spin-phonon relaxation rate for the H_2 (D_2) magnetization. Equation (1) is appropriate in the limit of negligible quadrupolar splitting of the H_2 (D_2) molecular-spin spectrum. In the limit of large quadrupole splittings only the first term in the second set of square brackets should be retained. In this case the formula is identical to the one for the relaxation of nuclear spins by paramagnetic impurities. As might have been anticipated, the relaxation rate arising from this mechanism is smaller than the rate from the first mechanism unless r is smaller than the separation of the nuclei in an H_2 (D_2) molecule. Therefore, this second mechanism does not compete effectively with the first.

(iii) The third relaxation mechanism considered is identical to the second, except that the coupling is quadrupolar instead of dipolar and thus the mechanism applies only to the relaxation of D. The calculation again is similar to the standard calculation¹² for spin relaxation via paramagnetic impurities, except that the quadrupole Hamiltonian is used rather than the dipolar Hamiltonian. In the limit of large quadrupole splittings the relaxation rate is

$$R = \frac{1}{\hbar^2} (Q_n Q_m e^2 / r^5)^2 (\frac{2}{5})^3 [F(\omega_0) + 2F(2\omega_0)], \quad (3)$$

where Q_n and Q_m are the quadrupole moments of

the D nuclei and D_2 molecule, respectively. In the limit of no quadrupole splitting there are eight additional terms in the square brackets involving sums and differences of ω_0 and ω_m . Again, this relaxation rate is smaller than that for the first process unless r is smaller than the separation of nuclei in an H_2 (D_2) molecule.

V. EXPERIMENTAL RESULTS AND ANALYSES

A. Spin-lattice relaxation

Figure 3 shows a doubly logarithmic plot of T_1 as a function of temperature for both protons (H) and deuterons (D) in α -Si:(D,H) at 14.4 MHz. There is no apparent minimum for T_1 (H) and the observed T_1 (D) is shorter than T_1 (H) at all temperatures at which both relaxation times were measured. The analysis that follows will conclude that the α -Si:(D,H) sample contains 2 orders of magnitude more molecular D_2 than H_2 , and that this fact accounts for the more rapid D relaxation. The proton relaxation T_1 (H) observed at 14.4 MHz will be found to arise both from relaxation to dilute o - H_2 and also from relaxation to an electronic paramagnetic impurity, which probably is oxygen.

The following discussion will use the notation $T_{1\alpha}$ (H) and $T_{1\alpha}$ (D) for the relaxation of H and D that is related to molecular H_2 and D_2 , respectively. $T_{1\beta}$ (H) and $T_{1\beta}$ (D) will represent H and D relaxation components that do not arise from molecular H_2 and D_2 . It will be assumed that the α and β relaxation processes are independent and that the relaxation rates $T_{1\alpha}^{-1}$ and $T_{1\beta}^{-1}$ are additive.

Figure 4 presents the T_1 (H) proton spin-lattice relaxation data at both 14.4 and 91.8 MHz. A sin-

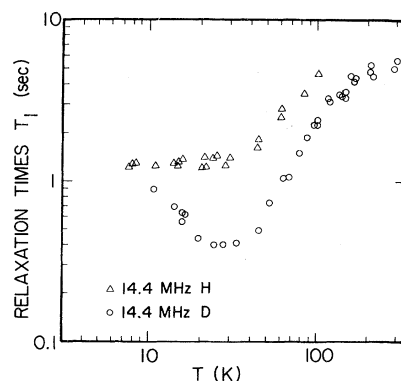


FIG. 3. 14.4-MHz spin-lattice relaxation times T_1 for H and D.

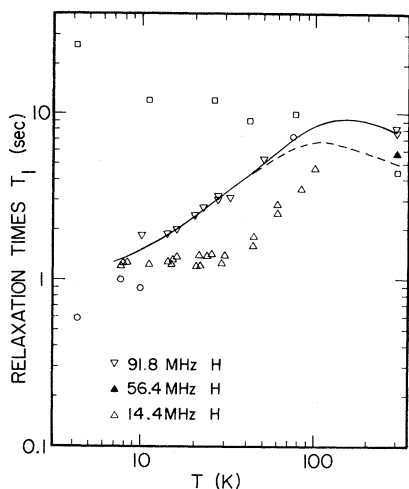


FIG. 4. Proton spin-lattice relaxation times T_1 at 14.4, 56.4, and 91.8 MHz in α -Si:(D,H). The circles indicate the oxygen-related $T_{1\beta}$ deduced from α -Si:H results (samples BNL94 and BNL95) reported (Ref. 13) by Carlos and Taylor and the squares indicate T_1 results for a sputtered α -Si:H sample (Ref. 14) that showed no H_2 -related T_1 minimum. The solid line is drawn through the present 91.8-MHz data. The dashed line indicates an estimated corresponding 14.4-MHz $T_{1\beta}$ component.

gle room-temperature $T_1(H)$ measurement at 56.4 MHz, reported for this sample by Reimer, Vaughan, and Knights⁹ is indicated by a solid triangle. There clearly is some variation in $T_1(H)$ with a Larmor frequency near 300 K, although the present 14.4-MHz measurements did not extend above 103 K.

The temperature dependence of $T_1(H)$ at 91.8 MHz suggests that the relaxation at this Larmor frequency arises primarily from the presence of oxygen in the sample. Carlos and Taylor¹³ have reported proton $T_1(H)$ data at 42.3 MHz on two Brookhaven National Laboratory plasma-deposited α -Si:H samples that differ only in their oxygen content. Their BNL95 sample was similar to sample BNL94 except for the addition of 1.5 at. % oxygen. The resulting T_1 reduction in sample BNL95 was greatest at low temperatures. Figure 4 includes (as open circles) four data points on the oxygen-related $T_{1\beta}(H)$ calculated as follows:

$$\frac{1}{T_{1\beta}(H)} = \frac{1}{T_1(\text{BNL95})} - \frac{1}{T_1(\text{BNL94})}. \quad (4)$$

The four $T_{1\beta}$ points agree with the general tem-

perature dependence of the present $T_1(H)$ at 91.8 MHz below 100 K. Street, Knights, and Biegelsen⁸ have indicated that the preparation conditions for the present sample make it likely that a significant oxygen contamination is present.

At temperatures above 100 K there is an additional temperature variation of $T_1(H)$, probably similar to the decrease with increasing T observed (Figs. 1 and 3) for the doublet fraction of the deuteron resonance and for the central fraction $T_1(D)$ at 14.4 MHz above 100 K. A straight line fitted to the doublet-fraction deuteron T_1 data at the top of Fig. 1 corresponds to a power-law temperature dependence $T_1 \propto T^{-\xi}$ with $\xi \approx 0.25$. This is consistent with the temperature dependence found for the proton T_1 in several α -Si:H samples. The squares in Fig. 4 show the 42.3-MHz proton $T_1(H)$ reported by Carlos, Taylor, Oguz, and Paul¹⁴ for a sputtered α -Si:H sample that did not exhibit a molecular- H_2 -related $T_1(H)$ minimum. A different power-law variation with $\xi \approx 1.4$ has been reported¹⁵ for quadrupolar relaxation in various glasses between 10 and 100 K.

It also appears that the 14.4-MHz $T_1(H)$ and $T_1(D)$ data (Figs. 3 and 4) for the present α -Si:(D,H) sample are limited at temperatures above 100 K by a T_1 relaxation mechanism that is well characterized by a temperature dependence similar to that of the data represented by squares in Fig. 4 and by solid triangles at the top of Fig. 1. We have chosen to regard the 91.8-MHz $T_1(H)$ data (Fig. 4) as primarily $T_{1\beta}(H)$, that is, as relaxation not related to molecular o - H_2 , and we have represented this relaxation by the solid line drawn in Fig. 4. The dashed line indicates a corresponding $T_{1\beta}(H)$ at 14.4 MHz, drawn to recognize the frequency dependence of T_1 evident near 300 K. In the following analysis the 14.4-MHz $T_{1\beta}(H)$ line will be used to correct the $T_1(H)$ data to obtain the $T_{1\alpha}(H)$ o - H_2 -related contribution to the 14.4-MHz proton relaxation.

The T_1 minima in the deuteron $T_1(D)$ results shown in Fig. 1 for the narrow unsplit DMR line clearly are dominated by deuteron relaxation to p - D_2 molecules. Nevertheless, both the 14.4- and 30-MHz $T_1(D)$ data show another limiting $T_{1\beta}(D)$ process at temperatures well below and above the T_1 minima. Since the proton $T_1(H)$ data show a significant $T_{1\beta}(H)$ relaxation contribution, it is reasonable to suppose the presence of such a component in the deuteron $T_1(D)$ results as well.

We fit the narrow-line $T_1(D)$ data of Fig. 1 to a $T_{1\alpha}(D)$ contribution related to molecular p - D_2 by the following procedure. We first fit the $T_1(D)$ data near the T_1 minima by means of rapid spin-

diffusion and spin-diffusion bottleneck terms

$$T'_{1\alpha}(\text{D}) = AT_1(\text{D}_2) + B. \quad (5)$$

The data fall below this fitted function at high and low temperatures, and so we calculate for each data point a residual relaxation contribution given by

$$\frac{1}{T'_{1\beta}(\text{D})} = \frac{1}{T_1(\text{D})} - \frac{1}{T'_{1\alpha}(\text{D})}. \quad (6)$$

We then slightly vary the parameters A and B seeking a residual set of $T'_{1\beta}(\text{D})$ points that follow a smooth function of T . Through these $T'_{1\beta}(\text{D})$ points we draw an averaged $T_{1\beta}(\text{D})$ line. We then use $T_{1\beta}(\text{D})$ to correct each original data point to get the molecular- D_2 -related component $T_{1\alpha}(\text{D})$,

$$\frac{1}{T_{1\alpha}(\text{D})} = \frac{1}{T_1(\text{D})} - \frac{1}{T_{1\beta}(\text{D})}. \quad (7)$$

The corrected $T_{1\alpha}(\text{D})$ points differ from the original $T_1(\text{D})$ points by only about 2% in the vicinity of the T_1 minima. The full set of $T_{1\alpha}(\text{D})$ points are then fitted by a slightly corrected $AT_1(\text{D}_2) + B$ expression to represent the deduced relaxation associated with deuteron relaxation via molecular $p\text{-D}_2$.

Figure 5 shows the results of such a procedure. The 14.4- and 30-MHz $T_{1\alpha}(\text{D})$ data points are those of Fig. 1, modified by the residual $T_{1\beta}(\text{D})$ functions shown by lines at the top of Fig. 5. The $T_{1\beta}(\text{D})$ lines have temperature dependences at low and high temperatures that are the same as those of the

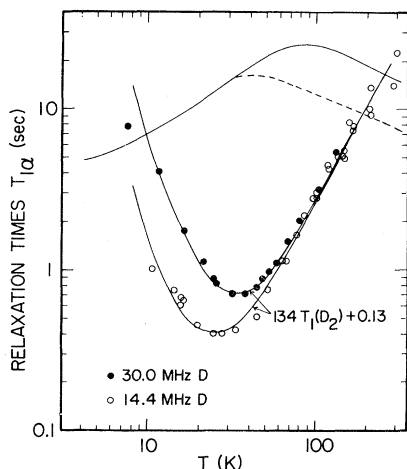


FIG. 5. Molecular-deuterium-related $T_{1\alpha}$ for D at 14.4 and 30.0 MHz. The fitted lines through the $T_{1\alpha}$ points correspond to $134T_1(\text{D}_2) + 0.13$ sec. The lines at the top of the figure indicate the $T_{1\beta}$ components used in the data separations at the two frequencies.

$T_{1\beta}(\text{H})$ lines indicated in Fig. 4. The solid lines in Fig. 5 indicate optimized fits to the plotted $T_{1\alpha}(\text{D})$ points and correspond to the molecular-paradeuterium-related relaxation

$$T_{1\alpha}(\text{D}) = 134T_1(\text{D}_2) + 0.13 \text{ sec}. \quad (8)$$

The calculations have assumed that the deuteron relaxation¹⁰ in dilute molecular $p\text{-D}_2$ in the $a\text{-Si}:(\text{D},\text{H})$ sample is characterized by electric field gradients of no symmetry, with $r=0$, and a characteristic temperature $\Theta_c = 40$ K. These are the same parameters that were found¹¹ to describe dilute $o\text{-H}_2$ in solid neon and argon and that have provided reasonable descriptions^{1,13} of proton relaxation in $a\text{-Si}:\text{H}$. The temperatures of the 14.4- and 30-MHz $T_{1\alpha}(\text{D})$ minima have been taken to be 25 and 34 K. The $T_{1\alpha}(\text{D})$ data above 100 K are independent of Larmor frequency and those on the low-temperature side of the T_1 minima are in good agreement with the anticipated ω_0^2 dependence.

It has not yet been shown by DMR measurements on $p\text{-D}_2$ in rare-gas solids that 40 K is an appropriate Θ_c for deuterium. However, far-infrared measurements reported¹⁶ on dilute solid mixtures $\text{H}_2\text{-Ar}$ and $\text{D}_2\text{-Ar}$ have shown a "resonant-mode" absorption at 22 cm^{-1} (~ 31 K) for both samples. Because of the lack of variation with hydrogen mass it has been speculated¹⁷ that the absorption arises from the formation of $\text{H}_2\text{-Ar}$ and $\text{D}_2\text{-Ar}$ molecules or that the absorption frequency reflects¹⁸ relaxation of the host lattice in the vicinity of the light impurity. There also are observed H_2 - and D_2 -related local-mode absorptions above the Debye frequency and these show¹⁶ the anticipated mass dependence.

In any event $\Theta_c = 40$ K provides a reasonable fit to the $T_1(\text{D})$ data of Fig. 5. Computer analyses indicate that the fit is noticeably degraded with $\Theta_c = 30$ and 50 K, but that the present limited data prevent the exclusion of $\Theta_c = 35$ or 45 K. The 14.4-MHz $T_{1\beta}(\text{H})$ line of Fig. 4 is now employed to correct the $T_1(\text{H})$ data points and to obtain the $T_{1\alpha}(\text{H})$ molecular- H_2 -related times shown in Fig. 6. These proton $T_{1\alpha}(\text{H})$ data have been fitted with the molecular-ortho-hydrogen-related relaxation expression

$$T_{1\alpha}(\text{H}) = 4590T_1(\text{H}_2) + 0.25 \text{ sec}. \quad (9)$$

Also shown for comparison are the 14.4-MHz $T_{1\alpha}(\text{D})$ data and fit of Fig. 5 and Eq. (8). Both sets of 14.4-MHz relaxation times show clear $T_{1\alpha}$ minima centered at 25 K. Both minima are well fitted by $\Theta_c = 40 \pm 5$ K. A consequence of Eq. (9) is that

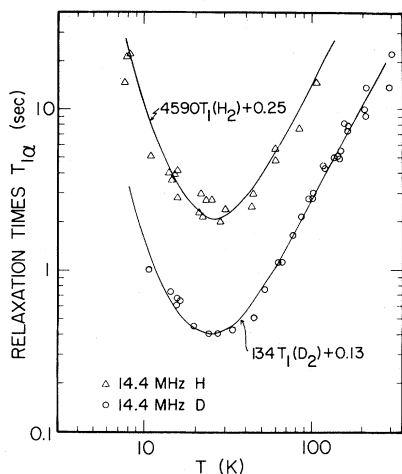


FIG. 6. $T_{1\alpha}$ for H and D at 14.4 MHz. The line through the D data is from Fig. 5 and is $134T_1(D_2)+0.13$ sec. The line through the H data is $4590T_1(H_2)+0.25$ sec. Both curves have minima at 25 K and are calculated for no symmetry, $r=0$, and $\Theta_c=40$ K.

at 91.8 MHz, $T_{1\alpha}(H)$ has a minimum of 15 sec near 54 K. This contribution has little effect on the 91.8-MHz $T_1(H)$ data of Fig. 4 and so the assumption that these results are primarily $T_{1\beta}(H)$ appears sound.

It now is feasible to calculate the molecular correlation frequencies Γ_2 for dilute o - H_2 and p - D_2 in the α -Si:(D,H) sample by using the $T_{1\alpha}$ data of Figs. 5 and 6, Eqs. (8) and (9), and the angular-averaged, no-symmetry, $r=0$ relaxation expression¹⁰

$$\frac{1}{T_1} = \frac{6}{5} \omega_d^2 [F_2(\omega_0) + 2F_2(2\omega_0)]. \quad (10)$$

Here $F_2(\omega) = \Gamma_2/(\omega^2 + \Gamma_2^2)$, $\omega_d(H_2) = 3.624 \times 10^5$ sec⁻¹, and $\omega_d(D_2) = 1.586 \times 10^5$ sec⁻¹.¹⁹

The Γ_2 values calculated for each $T_{1\alpha}$ point of Figs. 5 and 6 are shown in Fig. 7. Also shown for comparison are Γ_2 values calculated¹¹ from $T_1(H_2)$ data for dilute o - H_2 in solid neon and argon. The curved lines through the neon and argon results indicate Γ_2 was calculated¹¹ using a phonon-Raman process for molecular relaxation. The present results are more scattered, but some general features are evident. $\Gamma_2(T)$ for α -Si:(D,H) lie to the right of those for neon and argon, but in all three materials it is found that the low-temperature $\Gamma_2(T)$ data approach the expected T^7 asymptotic behavior with the neon data showing a clear T^7 regime. At high temperatures the α -Si results are more clearly T^2 than are those for argon, which in turn are more T^2

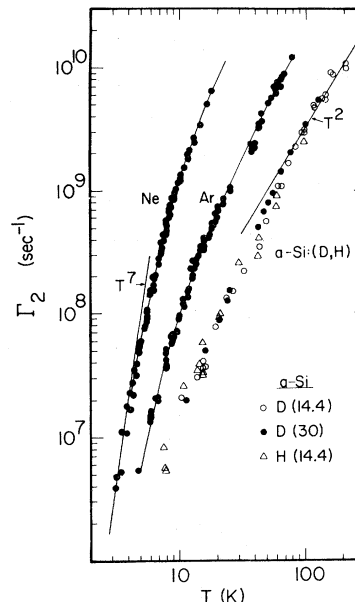


FIG. 7. Molecular correlation frequencies Γ_2 calculated [via Eq. (10)] for 14.4-MHz $T_{1\alpha}(H)$ and 14.4- and 30.0-MHz $T_{1\alpha}(D)$. For comparison, Γ_2 results are shown for dilute o - H_2 in solid neon and argon. The curved lines through these data correspond to a fitted phonon-Raman process for molecular relaxation. The straight lines indicate the anticipated T^7 and T^2 limiting behaviors at low and high temperatures, respectively.

than for neon. That is to say, the temperature range of the neon Γ_2 data extends only up to 18 K, which is significantly less than the common characteristic temperature $\Theta_c=40$ K. On the other hand, the argon data extended to 80 K and the α -Si:(D,H) data extended to 210 K, so that the T^2 behavior is better established in those cases. As anticipated, the α -Si:(D,H) $\Gamma_2(T)$ results are the same for 14.4 and 30 MHz and for both p - D_2 and o - H_2 .

B. Relaxation to molecular hydrogen

It is useful to compare the proton and deuteron $T_{1\alpha}$ results in both the rapid spin-diffusion and spin-diffusion bottleneck regimes. Analyses of the data of Figs. 5 and 6 have yielded Eqs. (8) and (9),

$$T_{1\alpha}(D) = 134T_1(D_2) + 0.13 \text{ sec},$$

$$T_{1\alpha}(H) = 4590T_1(H_2) + 0.25 \text{ sec}.$$

For no symmetry and $r=0$ the T_1 minima for protons in dilute o - H_2 and for deuterons in dilute p - D_2 are equal to $0.585\omega_0/\omega_d^2$. Thus at 14.4 MHz,

$T_{1\min}(\text{D}_2) = 2.11 \times 10^{-3}$ sec and $T_{1\min}(\text{H}_2) = 4.03 \times 10^{-4}$ sec, while at 30.0 MHz, $T_{1\min}(\text{D}_2) = 4.38 \times 10^{-3}$ sec. Equation (8) then yields for $T_{1\alpha}(\text{D})$ at 14.4 MHz, $0.28 + 0.13 = 0.41$ sec, and at 30.0 MHz, $0.59 + 0.13 = 0.72$ sec. Equation (9) yields for $T_{1\alpha}(\text{H})$ at 14.4 MHz, $1.85 + 0.25 = 2.10$ sec. Now at constant Lamor frequency Eq. (10) permits calculation of the ratio

$$\frac{T_1(\text{H}_2)}{T_1(\text{D}_2)} = \left[\frac{\omega_d(\text{D}_2)}{\omega_d(\text{H}_2)} \right]^2 = 0.192. \quad (11)$$

1. Rapid spin diffusion

Neglecting intermolecular EQQ interactions and assuming rapid spin diffusion among the H, $T_{1\alpha}(\text{H})$ will be longer than $T_1(\text{H}_2)$ by a ratio of spin heat capacities¹⁻³:

$$T_{1\alpha}(\text{H}) = T_1(\text{H}_2) \frac{n(\text{H})I(I+1)}{\frac{3}{4}n(\text{H}_2)S(S+1)}, \quad (12)$$

where $n(\text{H})$ and $n(\text{H}_2)$ are the number densities of hydrogen and H_2 molecules in the sample. The $\frac{3}{4}$ factor assumes that the experiments are made sufficiently quickly that the room-temperature ortho-para ratio is frozen in. (The conversion half-life has been measured⁴ in *a*-Si:H to be about two weeks at 4.2 K.) $I = \frac{1}{2}$ is the proton spin and $S = 1$ is the nuclear spin of *o*- H_2 . Thus Eq. (12) becomes

$$\frac{T_{1\alpha}(\text{H})}{T_1(\text{H}_2)} = \frac{n(\text{H})}{2n(\text{H}_2)}, \quad (13)$$

which equals 4590 according to Eq. (9). Thus our determination that $n(\text{H}) = 7$ at. % implies that $n(\text{H}_2) = 7.6 \times 10^{-6}$ (7.6 ppm or $3.8 \times 10^{17} \text{ cm}^{-3}$).

A similar analysis of $T_{1\alpha}(\text{D})$ associated with rapid spin diffusion to *p*- D_2 molecules yields the relation

$$T_{1\alpha}(\text{D}) = T_1(\text{D}_2) \frac{n(\text{D})I(I+1)}{\frac{1}{3}n(\text{D}_2)S(S+1)}, \quad (14)$$

where now $I = S = 1$ and the room-temperature para-ortho ratio of $\frac{1}{3}$ has been used. Thus Eq. (14) becomes

$$\frac{T_{1\alpha}(\text{D})}{T_1(\text{D}_2)} = \frac{3n(\text{D})}{n(\text{D}_2)}, \quad (15)$$

where $n(\text{D}_2)$ is the total molecular- D_2 number density in the weakly bound fraction. Equation (8) states that $T_{1\alpha}(\text{D})/T_1(\text{D}_2) = 134$, so the spin-count

result that $n(\text{D}) = 3$ at. % for the weakly bound fast-relaxing fraction corresponds to $n(\text{D}_2) = 670$ ppm, or $3.3 \times 10^{19} \text{ cm}^{-3}$.

Thus the molecular density ratio is

$$\frac{n(\text{D}_2)}{n(\text{H}_2)} = 88, \quad (16)$$

which reflects the D_2 -rich preparation environment in the vicinity of the cathode substrate. Equation (16) is probably a rather reliable result since the T_1 bottleneck contribution is only about 12% for protons and 30% for deuterons.

2. Spin-diffusion bottleneck

Assuming the room-temperature *o*- H_2 to *p*- H_2 and *p*- D_2 to *o*- D_2 ratios, the bottleneck relaxation rates are given by^{1,12}

$$\frac{1}{T_{1\alpha}(\text{H})} = 4\pi D_{\text{H}} \frac{3}{4} n(\text{H}_2) b_{\text{H}} \quad (17)$$

and

$$\frac{1}{T_{1\alpha}(\text{D})} = 4\pi D_{\text{D}} \frac{1}{3} n(\text{D}_2) b_{\text{D}}. \quad (18)$$

Here D_{H} and D_{D} are the spin-diffusion coefficients for the H and D, respectively, and the parameters b_{H} and b_{D} are the mean spacing between H_2 (D_2) and its nearest H (D) neighbors. We assume that $b_{\text{D}} = b_{\text{H}}$.

If we assume¹ that D_{H} and D_{D} are roughly independent of $n(\text{H})$ and $n(\text{D})$ in the strongly clustered *a*-Si: (D,H) sample, and if we also assume that there are no significant quadrupolar interference effects on D_{D} for the narrow-line phase, then

$$\frac{D_{\text{H}}}{D_{\text{D}}} = \frac{\gamma_{\text{H}}^2 \sqrt{I(I+1)}}{\gamma_{\text{D}}^2 \sqrt{S(S+1)}} = 42.44 \left[\frac{3/4}{2} \right]^{1/2} = 26.0. \quad (19)$$

Thus if $b_{\text{D}} = b_{\text{H}}$, one has the ratio

$$\left[\frac{T_{1\alpha}(\text{H})}{T_{1\alpha}(\text{D})} \right]_{\text{bottleneck}} = \frac{4 D_{\text{D}} n(\text{D}_2)}{9 D_{\text{H}} n(\text{H}_2)} = \frac{1}{58.5} \frac{n(\text{D}_2)}{n(\text{H}_2)}. \quad (20)$$

The observed bottleneck values of 0.25 and 0.13 sec

then yield the ratio

$$\frac{n(D_2)}{n(H_2)} = \frac{0.25}{0.13} 58.5 = 113, \quad (21)$$

which is in reasonable agreement with the rapid spin-diffusion result for the ratio of molecular densities $n(D_2)/n(H_2) = 88$.

If we had not assumed the spin-diffusion coefficients to be independent of $n(H)$ and $n(D)$ for the clustered sample, then for a dilute lattice one would anticipate²⁰

$$D_H \propto \frac{a^2}{T_2} \propto n(H)\gamma_H^2 \sqrt{I(I+1)} n(H)^{-2/3} \quad (22)$$

(where a is the mean proton spacing, about 4 Å). A similar anticipation for D_D shows that

$$\frac{D_H}{D_D} = 26.0 \left[\frac{n(H)}{n(D)} \right]^{1/3}.$$

Then the ratio $n(D_2)/n(H_2)$ is about 30% larger than Eq. (21).

In either case the deuteron bottleneck $T_{1\alpha}(D) = 0.13$ sec is within a factor of 2 of that for protons $T_{1\alpha}(H) = 0.25$ sec. This occurs, in spite of the smaller spin-diffusion coefficient for D, because of the D_2 concentration 2 orders of magnitude larger than that for H_2 . The molecular concentrations deduced from the rapid-relaxation regime probably are reliable since they depend [Eqs. (12) and (14)] only on the measured relaxation times and spin counts and on the well-established^{10,11} relaxation rates for dilute molecular hydrogen.

If we accept the rapid-diffusion result $n(H_2) = 3.8 \times 10^{17}$ cm⁻³ and use $b_H \approx 4 \times 10^{-8}$ cm, then Eq. (17) and the bottleneck $T_1(H) = 0.25$ sec yield $D_H \approx 2.8 \times 10^{-11}$ cm²/sec. This is a value some 30 times larger than that found appropriate in the analysis¹ of proton relaxation⁷ in a plasma-deposited *a*-Si:H sample prepared on a 250°C substrate. The difference may arise from different degrees of clustering or from other undetermined factors.

The preceding analyses are based on calculated proton and deuteron T_1 values in molecular *o*-H₂ and *p*-D₂, which are based on the assumption that there are large local electric field gradients with no symmetry. If in fact the electric field gradient (efg) at the molecular sites are small or have higher symmetry, then $T_1(H_2)$ and $T_1(D_2)$ can be smaller by as much as a factor of 4 (Ref. 10) than our calculated values. This in turn would decrease proportion-

ally the deduced molecular concentrations $n(H_2)$ and $n(D_2)$, while preserving their ratio. Given the interstitial nature of the probable H₂ (D₂) site and the probable trapping in microvoids,^{1,13} it is not likely that the efg have very high symmetry.

C. Transverse relaxation of the narrow DMR line

The open circles and solid dots near the bottom of Fig. 1 indicate the deuteron T_2 results for the 3-at. % D weakly bound phase. Spin-count calibrations indicate that $M_0 T$ is independent of temperature for this narrow-line fraction over the full data range. The T_2 data are drawn from a number of measurements at 14.4 and 30.0 MHz, including free-induction decays and Fourier transforms of free-induction decays.

Figure 8 shows the Fourier transforms of 30-MHz free-induction decays at three temperatures. The pulse repetition rate has been set to be high enough to saturate the long- T_1 doublet component. The remaining central line is nearly Lorentzian above 10 K and at 39 K shows a halfwidth at half maximum of 3170 sec⁻¹, corresponding to a Lorentzian $T_2 = 3.16 \times 10^{-4}$ sec. The magnetic field inhomogeneity of the 45.9-kG superconducting solenoid over the sample corresponds to a magnet $T_2^* = 1.5 \times 10^{-3}$ sec, so the magnet-corrected

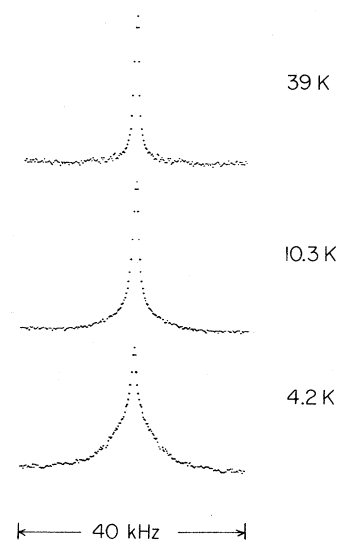


FIG. 8. Fourier transforms of 30.0-MHz narrow-component DMR free-induction decays at three temperatures. The displayed frequency interval is 40 kHz and the three resonances have been scaled to similar heights. The pulse repetition rate has been set high enough to saturate out the DMR doublet component.

39-K T_2 is 4.0×10^{-4} sec and is indicated in Fig. 1 as a solid dot.

The line broadens as the temperature is reduced and the magnet-corrected T_2 at 6.4 K is 1.5×10^{-4} sec, while that at 4.2 K is 1.3×10^{-4} sec. For these two coldest points the Lorentzian line-shape approximation is less valid and the definition of T_2 has become questionable. The open circles in Fig. 1 indicate deuteron T_2 values deduced from 14.4-MHz free-induction decays. For these measurements in a 12-in. electromagnet the magnet T_2^* correction is negligible. T_2 appears to be independent of magnetic field at the two fields employed.

The $T_2(D)$ data (open circles and solid dots) at the bottom of Fig. 1 show an approximately $T^{0.6}$ temperature dependence from 4.2 to 300 K, with perhaps a more rapid variation at higher temperatures. The line narrowing with increasing temperature is not associated with the onset of hydrogen atomic diffusion, which occurs¹³ above 500 K in typical plasma-deposited *a*-Si:H samples. Similarly, the narrowing does not seem to be phonon-related since the observed temperature dependence does not lie in the anticipated¹¹ T^7 to T^2 range.

Typical proton linewidths for *a*-Si:H samples²¹ show an approximately 3-kHz component corresponding to the weakly bound fraction and nearly independent of H concentration in the highly clustered samples. Since the weakly bound fraction in the present sample contains 3 at. % D and perhaps 1 at. % H, both D-D and D-H dipolar interactions are significant. The D dipolar rigid-lattice linewidth should be about 11% of the proton linewidth, giving an anticipated dipolar $\Delta\nu(D)$ about 300 Hz for the weakly bound deuterium (WBD) fraction. The observed 130- μ sec T_2 at 4.2 K corresponds (Fig. 8) to a $\Delta\nu_{1/2,1/2}$ linewidth of 1.2 kHz, and thus to a value about a factor of 4 too large to be dipolar in origin. It is probable that the 4.2-K line shape primarily reflects freezing out into various static quadrupolar interaction configurations. This conclusion is also supported by the observability of a 90° - τ - $90^\circ_{90^\circ}$ quadrupole echo for the WBD component. At 4.2 K the envelope of this WBD quadrupole echo corresponds to a T_2 of 1.4 msec (square in Fig. 1).

Reimer, Vaughan, and Knights⁹ (RVK) have reported proton T_{1y} values that decrease with decreasing temperature for proton NMR measurements in a similar but nondeuterated *a*-Si:H sample. The proton T_{1y} data correspond to the decay of magnetization when homonuclear dipolar interactions were suppressed by an eight-pulse cycle. The RVK T_{1y} decays were nonexponential and were analyzed via

initial and final decay times. The $T_{1y}(T)$ variations were analyzed in terms of exponential activation energies near 250 cal/mole. The RVK T_{1y} results are indicated as triangles at the upper left of Fig. 9 and have been taken from Fig. 2 of their paper.

Also shown in Fig. 9 are the WBD narrow-line $T_2(D)$ data of Fig. 1, here replotted as $\ln T_2$ vs $1000/T$. If these data reflect exponentially activated narrowing, then clearly at least two regimes are apparent. Above 100 K there is a steeper exponential corresponding to an activation of about 500 cal/mole (0.02 eV/atom). Below 100 K, our T_2 results show a dramatically different temperature variation that indicates a much smaller activation energy near 10 cal/mole (4×10^{-4} eV/atom). Also shown as a solid curved line in Fig. 9 is a $T^{0.6}$ power-law fit to the present data. Clearly both the $T_2(D)$ and the $T_{1y}(H)$ results may in fact be described by a power law rather than by an exponentially activated temperature variation. RVK speculated⁹ that the approximately 250-cal/mole activation energies of their T_{1y} data reflected the presence of hydrogen-containing local disorder modes. The present $T_2(D)$ data may indicate the presence of two activation energies as the central narrow-line components are progressively frozen out into differing quadrupolar rigid-lattice configurations. However, it also is possible that the data are more properly described by a $T^{0.6}$ temperature variation whose origin is at present not understood.

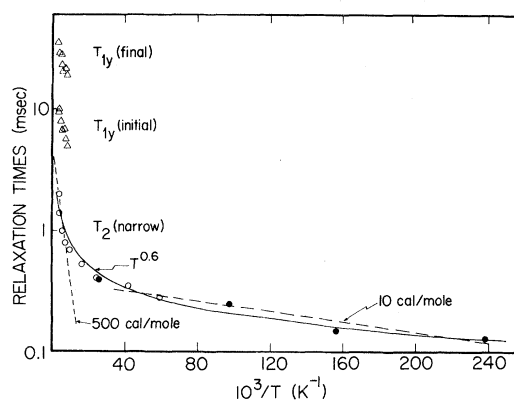


FIG. 9. Narrow-component DMR $\ln T_2$ data of Fig. 1 plotted vs reciprocal temperature. The dashed lines correspond to activation energies of 500 cal/mole (0.02 eV/atom) and 10 cal/mole (4×10^{-4} eV/atom). The triangles indicate T_{1y} results reported for a similar *a*-Si:H sample by a Reimer, Vaughan, and Knights (Ref. 9). The curved solid line indicates a $T^{0.6}$ power-law fit to the DMR T_2 data.

D. Quadrupole-split doublet

The rapid oscillations in the slow repetition-rate free-induction decays of Fig. 2 correspond to the presence of a doublet-split DMR component. A large rapidly decaying initial component of each decay signal is obscured in Fig. 2 by transients associated with the rf pulse. The complete DMR signal is observed via the shapes of $90^\circ\text{-}\tau\text{-}90^\circ_{90^\circ}$ quadrupole echoes. Figure 10 shows Fourier transforms of 30-MHz deuteron quadrupole echoes in *a*-Si:(D,H) at 39 and 4.2 K. The transforms have been taken for signals beginning at time 2τ (the echo peak) and the resonance lines plotted in Fig. 10 correspond to the transforms of the digital averages of 200 echo sweeps at 39 K and 16 sweeps at 4.2 K. The 39-K trace represents 10 h of digital signal averaging. The full spectral width displayed is 250 kHz.

The full splitting between main peaks of the doublet is 66 ± 1.0 kHz. The doublet-component signal area corresponds to 21-at. % D, in agreement with the anticipated fraction of TBD. The 66-kHz deuteron splitting is too large to be dipolar in origin. The calculated line drawn in Fig. 10 shows the excellent fit of a quadrupolar Pake doublet function¹² calculated for a powder-averaged spin-1 system with an axial field gradient and zero-asymmetry parameter.²² The splitting apparently arises from the electric field gradient associated with a bond to a single nearby silicon atom. The 21-at. % doublet TBD fraction is particularly distinct from the 3-at. % WBD narrow line, since the two components have spin-lattice relaxation times T_1 , which differ by a factor of about 200 at 39 K (Fig. 1). Deuteron spin diffusion to molecular D_2 impurities may be much reduced by the static quadrupole interaction in the doublet TBD phase.

Spin-lattice relaxation times T_1 associated with the TBD doublet component are shown at the top of Fig. 1. The slow decrease of T_1 with increasing temperature is similar to that observed for H in *a*-Si:H samples that do not show a T_1 minimum (Fig. 4).¹⁴ In the present sample the temperature variation is also similar to that part of the WBD narrow-line relaxation that does not arise from the presence of molecular deuterium or oxygen (Figs. 4 and 5).

For an axial gradient and $H_{\text{Zeeman}} \gg H_{\text{quad}}$ the energy levels are given¹² (in first order) by

$$E_Q = \frac{eqQ}{4I(2I-1)} [3m^2 - I(I+1)] \left[\frac{3\cos^2\theta - 1}{2} \right], \quad (23)$$

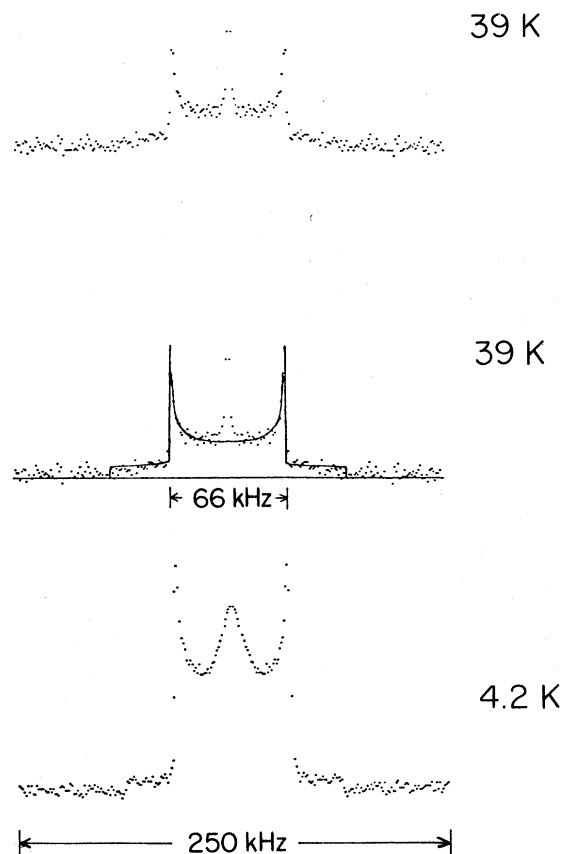


FIG. 10. Fourier transforms of 30.0-MHz DMR $90^\circ\text{-}\tau\text{-}90^\circ_{90^\circ}$ quadrupole echoes at 39 and 4.2 K. The displayed frequency interval is 250 kHz and the resonance doublet has a full-width splitting of 66 ± 1.0 kHz. The lines in the center figure indicate the fit of an $\eta=0$ quadrupolar doublet function to the data. Narrow-component DMR signals similar to those of Fig. 8 are visible at the center of the traces and correspond to 3-at. % D, while the doublet component corresponds to 21-at. % D.

where the symbols have their usual meanings and where we are using the notation that the field-gradient tensor component $V_{zz}=q$ (rather than eq). Thus the full splitting between the $\theta=\pi/2$ main peaks is, for $I=1$,

$$\Delta\nu = \frac{3}{4} \frac{eqQ}{h}. \quad (24)$$

In the present case $\Delta\nu$ is observed to be 66 ± 1.0 kHz. Thus the deuteron quadrupole coupling constant for the TBD phase is

$$\nu_q = \frac{eqQ}{h} = 88 \pm 1.3 \text{ kHz} . \quad (25)$$

With the use of the deuteron quadrupole moment $eQ = 2.738 \times 10^{-27} e \text{ cm}^2$, Eq. (25) implies an electric field gradient at the deuterons corresponding to

$$q = (2.13 \pm 0.02) \times 10^5 \text{ dyn/cm} . \quad (26)$$

Infrared-absorption measurements⁵ on *a*-Si:H samples that had been deposited on room-temperature substrates have yielded stretching-mode absorptions at reduced wave numbers between 2000 and 2200 cm^{-1} . These have been identified with structures SiH, SiH₂, (SiH₂)_n, and SiH₃. For deuterated samples the SiD stretching mode was shifted down to 1460 cm^{-1} . There are approximately 5% changes in the stretching-mode spectral frequencies for samples prepared with different plasma rf power levels.²³ For the present sample, prepared in a D₂-rich atmosphere, it is perhaps reasonable to anticipate significant amounts of structures SiD, SiD₂, and (SiD₂)_n.

It has been shown²⁴ that simple force-constant models are not sufficient to provide a quantitative description of the ir spectra of SiH, SiH₂, and SiH₃ groups in amorphous networks. Nevertheless, it is interesting to note that a linear relationship has been demonstrated between deuteron quadrupole coupling constants and stretching force constants calculated for diatomic molecules,^{25,26} and for hydrogen-bonded systems.^{27,28} The calculated ν_q for the SiD molecule is 92.6 kHz, which is expected to be reduced²⁸ by about 5% for (SiD)_n and large *n*. The result of Mokarram and Ragle²⁶ is that (in atomic units) the force constant is 1.127 times the field gradient at the deuteron.

If such a relationship is valid in *a*-Si, then our gradient result, Eq. (26), implies a stretching force constant

$$k = (2.40 \pm 0.02) \times 10^5 \text{ dyn/cm} . \quad (27)$$

This result compares very well with the stretching force constants calculated from the observed ir absorptions in *a*-Si:H that range from 2.29×10^5 dyn/cm (2000 cm^{-1}) to 2.77×10^5 dyn/cm (2200 cm^{-1}). Accepting the conversion coefficient determined from diatomic molecules, the ir absorption corresponding to our quadrupole doublet result, Eq. (25), would occur at $2050 \pm 15 \text{ cm}^{-1}$. Thus the quadrupole split resonance doublet of Fig. 10, observed for the tightly bound deuterium (TBD) phase in *a*-Si, corresponds to the silicon-hydrogen bond associated with the reported stretching-mode ir absorptions.

The 1.5% uncertainty in $\Delta\nu$, ν_q , and *k* compares favorably with that achieved in the ir measurements. The uncertainty in the present result arises from the apparently finite slope of the data points just outside the main $\theta = \pi/2$ peaks. The signals in Fig. 10 reduce by a factor of 2 over a frequency interval of about 500 Hz. This may reflect a distribution of SiD configurations and quadrupolar couplings. Dipolar broadenings can affect deuteron quadrupole echoes. However, for dipolar interactions that are small compared to quadrupole splittings, the Fourier transform of a $90^\circ\text{-}\tau\text{-}90^\circ_{90^\circ}$ quadrupole echo yields a less distorted quadrupolar spectrum²⁹ than those from other two-pulse echo sequences.

Stretching-mode infrared absorptions have been observed in a number of amorphous hydrides³⁰⁻³⁴ including those of Si, Ge, As, B, and C, as well as in a variety of alloys. The preceding analysis makes it possible to estimate the deuteron quadrupole coupling constants that may be expected to characterize DMR experiments on tightly bound deuterium in these materials. Table I lists some of these reported ir absorptions and the corresponding quadrupolar coupling coefficients. The anticipated C-D ν_q values near 180 kHz are in excellent agreement with the 182-kHz average of 58 deuterium coupling con-

TABLE I. Quadrupole coupling constants estimated from infrared-absorption data in amorphous hydrides.

	Stretching-mode absorption (cm^{-1})		ν_q (kHz)
GeH	1855, 1976 ^a	GeD	72, 82
AsH	1975 ^b	AsD	82
BH	2560 ^c	BD	138
CH	2890, 2945 ^d	CD	176, 182

^aReference 30.

^bReference 31.

^cReferences 32 and 33.

^dReference 34.

stants tabulated³⁵ from DMR measurements on 39 C-D fragments in various materials. It is to be expected that the actual $k(q)$ relationship for deuterons in amorphous semiconductors will differ somewhat from the diatomic molecule result²⁶ used above.

The calculated²¹ rigid-lattice H-H dipolar broadenings for some SiH configurations correspond to proton NMR full widths at half maximum: SiH₂ 13.6 kHz, (SiH₂)_n 17.1 kHz, and SiH₃ 19.2 kHz. For SiD species the corresponding widths scale as $\gamma^2\sqrt{I(I+1)}$, which is a factor of 26 [Eq. (19)]. Thus the D-D broadenings might range from 520 to 740 Hz, plus any contributions from ²⁹Si and ¹H (which probably are significant).

The observed quadrupolar doublet splitting and the doublet resonance line shape of Fig. 10 are independent of temperature over the full range of doublet observation from 4.2 to 160 K. The envelope of doublet-component quadrupole echoes observed as the pulse separation τ is varied gives a time constant $T_2=1.5$ msec, which also does not vary with temperature (triangles in Fig. 1). A single measurement at 4.2 K of the quadrupole echo envelope for the weakly bound phase unsplit narrow resonance line gave $T_2=1.4$ msec (square in Fig. 1) for that component as well. The observed echo envelope time constants may reflect the dipolar broadenings estimated above.

In plasma-deposited *a*-Si:H samples it usually is found^{6,36} that both the broad and narrow proton resonance lines have widths that are independent of temperature up to well above room temperature and that reflect the substantial clustering of H in both the tightly bound hydrogen and weakly bound hydrogen fractions. The present deuteron T_2 data in *a*-Si:(D,H) are insufficient for a detailed analysis, but it is probable that the dipolar parts of the deuteron transverse rates $1/T_2$ are also essentially independent of temperature from 4.2 to 200 K for both the doublet TBD and the narrow WBD fractions of the sample. However, there may be a significant difference (Figs. 8 and 10) between the 4.2-K transforms of the narrow component free-induction decay (FID) and quadrupole echo. It may be that the FID narrow-line transform is a composite corresponding to a 1.5-msec (~ 100 -Hz) dipolar line and a broader quadrupolar base. If the temperature dependence of T_2 (narrow) below 200 K in Fig. 1 is associated entirely with quadrupolar broadening and if there is a temperature-independent dipolar $T_2\approx 1.5$ msec, then the quadrupolar T_2 can be fitted by $T^{-\xi}$ with $\xi\approx 0.74$ instead of the 0.6 employed in Fig. 9.

VI. CONCLUSIONS

Spin-lattice relaxations of H and of the narrow-line weakly bound D fraction in an *a*-Si:(D,H) sample display components which proceed via molecular *o*-H₂ and *p*-D₂ impurities. The sample contains 2 orders of magnitude more D₂ than H₂, with the D₂ concentration similar to H₂ concentrations in other plasma-deposited *a*-Si:H samples. Both rapid spin-diffusion and spin-diffusion-bottleneck terms are evident in the T_1 (H) and T_1 (D). The terms correspond to similar ratios of D₂ and H₂ concentrations and the relaxation analyses are self-consistent.

Several competing relaxation mechanisms involving molecular hydrogen are considered and rejected in favor of the process previously described¹⁰ in which the H (D) nuclear magnetization diffuses to the nuclear spins of H₂ (D₂) molecules, which in turn relax to the lattice via the molecular angular momentum. Calibrated DMR spin counts indicate that the clearly distinguishable narrow and doublet deuteron resonances are associated, respectively, with the weakly bound and tightly bound deuterium (and hydrogen) fractions of the sample. This conclusion is also consistent with the fact that the largely quadrupolar linewidth of the narrow resonance at 4.2 K is significantly less than the doublet quadrupole splitting.

The transverse relaxation time for the narrow-line WBD fraction shows an approximately $T^{0.6}$ temperature dependence that, alternatively, may reflect a double-exponential Arrhenius behavior with activation energies near 0.02 and 4×10^{-4} eV/atom. The DMR quadrupole resonance doublet component corresponds to a quadrupole coupling constant 88 ± 1.3 kHz in the TBD phase. The doublet splitting corresponds well with silicon-hydrogen bond force constants deduced from reported infrared vibrational stretching-mode absorptions near 2100 cm^{-1} .

ACKNOWLEDGMENTS

We wish to thank J. Zesch for taking some of the relaxation data. The authors have benefited from conversations with R. Fisch, D. P. Grimmer, J. C. Knights, J. A. Reimer, P. C. Taylor, and D. R. Torgeson. We are grateful to W. E. Carlos and P. C. Taylor for providing us with tables of some of their *a*-Si:H proton relaxation data. This work was supported in part by the NSF Division of Materials Research under Grants Nos. DMR 80-10818 and DMR 8204166. One of us (D.J.L.) has benefited from a Washington University fellowship and a Xerox Corporation fellowship.

- ¹M. S. Conradi and R. E. Norberg, *Phys. Rev. B* **24**, 2285 (1981).
- ²M. Bloom, *Physica (Utrecht)* **13**, 767 (1957).
- ³W. N. Hardy and J. R. Gaines, *Phys. Rev. Lett.* **17**, 1278 (1966).
- ⁴W. E. Carlos and P. C. Taylor, *Phys. Rev. B* **25**, 1435 (1982).
- ⁵J. C. Knights and G. Lucovsky, in *Critical Reviews in Solid State and Materials Sciences*, edited by D. E. Schuele and R. W. Hoffman (CRC, Boca Raton, Fla., 1980), Vol. 9, p. 210.
- ⁶J. A. Reimer, R. W. Vaughan, and J. C. Knights, *Phys. Rev. Lett.* **44**, 193 (1980).
- ⁷W. E. Carlos and P. C. Taylor, *Phys. Rev. Lett.* **45**, 358 (1980).
- ⁸R. A. Street, J. C. Knights, and D. K. Biegelsen, *Phys. Rev. B* **18**, 1880 (1978).
- ⁹J. A. Reimer, R. W. Vaughan, and J. C. Knights, *Phys. Rev. B* **23**, 2567 (1981).
- ¹⁰P. A. Fedders, *Phys. Rev. B* **20**, 2588 (1979).
- ¹¹M. S. Conradi, K. Luszczynski, and R. E. Norberg, *Phys. Rev. B* **20**, 2594 (1979).
- ¹²A. Abragam, *The Principles of Nuclear Magnetism* (Oxford University Press, London, 1961).
- ¹³W. E. Carlos and P. C. Taylor, *Phys. Rev. B* **26**, 3605 (1982).
- ¹⁴W. E. Carlos, P. C. Taylor, S. Oguz, and W. Paul, in *Tetraedrally Bonded Amorphous Semiconductors (Carefree, Arizona)*, A Topical Conference on Tetraedrally Bonded Amorphous Semiconductors, edited by R. A. Street, D. K. Biegelsen, and J. C. Knights (AIP, New York, 1981), p. 67.
- ¹⁵T. L. Reinecke and K. L. Nagi, *Phys. Rev. B* **12**, 3476 (1975).
- ¹⁶J. de Remigis and H. L. Welsh, *Can. J. Phys.* **48**, 1622 (1970); R. J. Krieglner and H. L. Welsh, *ibid.* **46**, 1181 (1968).
- ¹⁷S. S. Cohen, *Chem. Phys. Lett.* **18**, 369 (1973).
- ¹⁸A. S. Barker, Jr. and A. J. Sievers, *Rev. Mod. Phys.* **47**, Suppl. No. 2, S1 (1975).
- ¹⁹N. F. Ramsey, *Molecular Beams* (Oxford University Press, London, 1956), p. 235.
- ²⁰G. R. Khutsishvili, *Usp. Fiz. Nauk* **87**, 211 (1965) [*Sov. Phys.—Usp.* **8**, 743 (1966)].
- ²¹J. A. Reimer, R. W. Vaughan, and J. C. Knights, *Phys. Rev. B* **24**, 3360 (1981).
- ²²R. G. Barnes and J. W. Bloom, *J. Chem. Phys.* **57**, 3082 (1972).
- ²³G. Lucovsky, R. J. Nemanich, and J. C. Knights, *Phys. Rev. B* **19**, 2064 (1979).
- ²⁴J. C. Knights, G. Lucovsky, and R. J. Nemanich, *Philos. Mag. B* **37**, 467 (1978).
- ²⁵L. Salem, *J. Chem. Phys.* **38**, 1227 (1963).
- ²⁶M. Mokarram and J. L. Ragle, *J. Chem. Phys.* **59**, 2770 (1973).
- ²⁷R. Blinc and D. Hadzi, *Nature (London)* **212**, 1307 (1966).
- ²⁸J. W. Clymer, N. Goldstein, J. L. Ragle, and E. L. Reed, Jr., *J. Chem. Phys.* **76**, 4535 (1982).
- ²⁹N. Boden, S. M. Hanlon, Y. K. Levine, and M. Mortimer, *Chem. Phys. Lett.* **57**, 151 (1978).
- ³⁰G. A. N. Connell and J. R. Pawlik, *Phys. Rev. B* **13**, 787 (1976).
- ³¹J. C. Knights, *Bull. Am. Phys. Soc.* **23**, 295 (1978).
- ³²C. C. Tsai, *Phys. Rev. B* **19**, 2041 (1979).
- ³³N. A. Blum, C. Feldman, and F. G. Satekiewicz, *Phys. Status Solidi A* **41**, 481 (1977).
- ³⁴H. Wieder, M. Cardona, and C. R. Guarnieri, *Phys. Status Solidi B* **92**, 99 (1979).
- ³⁵H. H. Mantsch, H. Saito, and I. C. P. Smith, *Prog. Nucl. Magn. Reson. Spectrosc.* **11**, 211 (1977).
- ³⁶J. A. Reimer, R. W. Vaughan, and J. C. Knights, *Solid State Commun.* **37**, 161 (1981).